Chinese Journal of Chemical Engineering 77 (2025) 135–143

Contents lists available at ScienceDirect

Chinese Journal of Chemical Engineering

journal homepage: www.elsevier.com/locate/CJChE

Full Length Article

Green synthesis of carbon dots by microflow method and their application as sunscreen agent

Ziyang Li, Zhikun Miao, Jie Shen, Jing Wang, Liangliang Lin*

Key Laboratory of Synthetic and Biological Colloids, Ministry of Education, School of Chemical and Material Engineering, Jiangnan University, Wuxi 214122, China

ARTICLE INFO

Article history:
Received 1 July 2024
Received in revised form
6 September 2024
Accepted 10 October 2024
Available online 19 November 2024

Keywords:
Carbon dot
Microflow synthesis
Sunscreen agent
Optimization
Nanoparticles
Chemical processes

ABSTRACT

Sunscreen agents derived from plants have been regarded as promising alternatives to artificial compounds. In this work, carbon dots (CDs) were prepared from carrot juice *via* a continuous microflow-based approach, where the influence of process parameters was studied and optimized. Complimentary characterization revealed the CDs not only have small size, narrow size distribution, and good water solubility, but also have abundant functional groups as well as excellent UV absorption performance. Relying on these properties, the CDs were used as UV absorbers, suggesting they have strong long-term UV absorption ability over a broad pH range. The UV-absorption properties of the CDs were confirmed by incorporating the CDs in polyvinyl alcohol (PVA) to get C-CDs@PVA films of different thickness, in which significantly enhanced UV absorption performance was observed. Besides, the sun protection performance is also related to the film thickness. Afterwards, the practical application of the CDs was evaluated by adding them in a typical skin cream. With the addition of the CDs, the cream has drastically reduced UV transmittance in both UVA and UVB regions, and exhibits better UV absorption performance than commercial sunscreen agents. The CDs also demonstrated low cytotoxicity and high DPPH radical scavenging activity, making them promising as green sunscreen absorbers. This work is expected to provide a guidance for the development of green and effective natural sunscreen agents *via* microflow-based method.

1. Introduction

Excessive exposure to ultraviolet (UV) radiation can be hazardous and may cause painful sunburns. The use of sunscreen, by reflecting and scattering UV radiation, is considered as an effective means to protect skin from UV radiation. Currently there are two major types of sunscreen agents: organic and inorganic [1]. The former one often uses organic compounds such as benzophenones, octocrylene, avobenzone, and *p*-aminobenzoic acid derivatives, *etc.* to absorb the UV radiation, while the latter one typically relies on zinc oxide or titanium dioxide to reflect UV rays [2]. Despite remarkable progress has been achieved in the development of sunscreens with customized properties, limitations also exist. For instance, organic agents can trigger skin irritations or allergic reactions when in contact with the skin. Some agents may even penetrate the skin and cause tissue damage and health risks [3]. As to inorganic agents, they tend to suffer from the whitening effect, low water solubility, low stability, and low transparency [4]. In addition, they can affect the epidermal layer of the skin or the internal organs *via* the respiratory tract.

Natural sunscreen agents, especially from plants, have been recognized as promising alternatives to traditional sunscreen agents to absorb or block UV radiation. Compared to artificial sunscreens, they have less skin toxicity and irritation as well as high environmental friendliness [5]. Besides, many natural compounds from plants have the capability to capture free radicals, thus endowing the sunscreen with antioxidant properties [6]. For instance, the presence of phenolic compounds, ketones, and intramolecular oxygen bonds in lignin makes it a good candidate as UV blocker and antioxidant [7]. Many seeds are rich in polyphenolic compounds like flavonoids and phenolic acids. They are well known for their antioxidant and anti-photo aging activities, and can be used to formulate sunscreens with antioxidant properties [8].

* Corresponding author.
E-mail address: linliangliang@jiangnan.edu.cn (L. Lin).

https://doi.org/10.1016/j.cjche.2024.10.008

In recent years, considerable effort has been dedicated to incorporating carbon dots (CDs) into different materials to endow them with new properties [9]. Due to the n-π* transition of the carbonyl groups and π-π* transition of the aromatic C=C bonds, CDs possess excellent UV absorption properties. Besides, the high water solubility as well as nontoxicity of CDs makes them promising in the field of life science, such as bio-imaging, bio-labels, *etc* [10,11]. Patil *et al.* [12] prepared CDs from waste tea dregs by hydrothermal method, and then used them to prepare transparent PVA@CDs composite films through solvent casting method. The obtained films were successful in blocking 100% of UVC and UVB rays, while 20% to 60% of UVA rays. Xu *et al.* [13] synthesized full UV-absorbing CDs from citric acid and 3-aminoquinoline, and mixed with PVA to get transparent sunscreen umbrella. No doubt, the above works reveal CDs can be applied for UV protection. However, when it comes to CDs synthesis, traditional approaches rely on labor- and energy-consuming selection of reagents and experimental conditions. Meanwhile, toxic chemical reagents or solvents are inevitably involved, which may have hazardous effects on human health and environment [14].

Microflow-based synthesis, due to the advantages like continuous operation, large specific surface area, and uniform residence time distribution, is considered to be an alternative to traditional batch processing [15]. In this study, small sized CDs of good water solubility were continuously prepared from carrot juice (C-CDs) *via* microflow method, without using toxic chemical reagents or solvents. The results showed the C-CDs not only have full-band UV absorption properties, but also offer consistent UV protection over a broad pH range. The C-CDs were then applied in preparing C-CDs@PVA films, reconfirming their excellent UV absorption performance. Furthermore, the microflow-prepared C-CDs were added in skin creams to evaluate their practical applications, suggesting they have good UV-shielding effect, biocompatibility, and antioxidant activity.

2. Materials and Methods

2.1. Materials

Carrot juice (Kagome, Japan) was purchased from a local supermarket. Octocrylene (OCT, ≥95%), octylmethoxycinnamate (OMC, ≥97%), glyceryl monostearate (≥90%), citric acid (≥98.0%), and stearic acid (≥98.0%) were purchased from Beijing InnoChem Science & Technology Co., Ltd. 1,1-Diphenyl-2-picrylhydrazine (DPPH, ≥99.5%) was purchased from Worthington Co., Ltd (U.S.). Avobenzone (AVB, ≥98.0%), 2-ethylhexyl salicylate (EHS, ≥98.0%), 1-hexadecanol (≥98.0%), 1,2-dihydroxypropane (≥99.5%), NaOH (AR), sodium dihydrogen phosphate (≥99.0%), sodium carbonate (≥99.8%), sodium bicarbonate (≥99.0%), methanol (≥99.5%), and 1,4-dioxane (≥99.7%) were purchased from Sinopharm Group Chemical Reagent Co., Ltd. Ethylhexyl methoxycinnamate (EHMC, ≥97.0%) and diethylaminohydroxybenzoyl hexyl benzoate (DHHB, ≥95.0%) were purchased from Shanghai Macklin Co., Ltd. The aqueous solution was prepared using deionized water with resistivity over 18 MΩ.

2.2. Preparation of C-CDs, C-CDs@PVA films, and sunscreen cream

In this work, carbon dots were synthesized using a microflow setup (Fig. S1, Supplementary Material). The detailed configuration of the setup can refer to our previous work [11]. In brief, it mainly consists of a plunger pump (Xingda 2 PB-1040II), an oil bath (Jinda DF-II), and a stainless-steel capillary (O.D. = 3.0 mm, I.D. = 2.0 mm, effective length = 4.2 m). In a typical procedure, 20 ml of carrot juice was added in 80 ml of deionized water at room temperature, stirred, and filtered with a 0.22 μm filter as the stock solution. The solution was then delivered into the capillary by the plunger pump at fixed rates, of which the reaction temperature and the residence time can be controlled by the oil bath and the pump respectively. After a desired processing time, the solution containing CDs was collected and filtered through 0.22 μm Millipore membranes for further characterization, or freeze-dried to obtain solid CDs. Systematic experiments have been performed to study the influence of the reaction temperature and residence time on the products. For convenience, the derived products were denoted as C-CDs-*x*-*y*, where *x* represents the reaction temperature, *y* represents the residence time.

C-CDs@PVA films were prepared using the solvent casting method. 1.5 g of polyvinyl alcohol was mixed with the C-CDs, and then dissolved in 30 ml of deionized water under stirring at 90 °C for 1 h to obtain PVA and C-CDs@PVA. Afterwards, 5 mlL of the mixed solution was dropped in a petri dish (diameter = 9.0 cm) and dried at 50 °C for 4 h to obtain C-CDs@PVA films. In this work, CDs of different concentrations (0–0.5 $mg \cdot ml^{-1}$) were added, and the derived C-CDs@PVA films were denoted as PVA, C-CDs@PVA-*z*, where *z* represents the concentration of the CDs. To assess the ultraviolet absorption performance of the C-CDs, skin cream was prepared according to the formula (Table S1) as the base [16]. Then, the cream was mixed with CDs of different contents to get sunscreens of different UV absorption properties.

2.3. Characterization

TEM characterization was performed on a JEM-2100Plus transmission electron microscope (FEI Company). Raman spectrum was recorded using a Renishaw inVia spectrometer (Gloucestershire) equipped with a confocal Leica microscope and a 532 nm excitation laser. X-ray diffraction (XRD) patterns were collected by a diffractometer (Bruker AXS GmbH, D8 Advance) using Cu-K_α radiation (K_α = 0.154056 nm) in the 2θ range of 10°–80°. The functional groups of the CDs were analyzed by a Nicolet 6700 Fourier-transform infrared spectrometer (FTIR, Seymour Fisher Technology Co., Ltd.). XPS characterization was carried out on a Kratos Axis Supra X-ray photoelectron spectrometer (Shimadzu Kratos Inc.) using monochromatic Al-K_α radiation (1486.6 eV). UV-Vis spectra in both absorbance and transmittance modes were recorded by a TU-1950 spectrophotometer (Beijing General Analysis General Co., Ltd.). Photoluminescence (PL) spectra were recorded on a Cary Eclipse spectrophotometer (Varian Co., Ltd.). The fluorescence decay curves were acquired using a LifeSpec II ultrafast time-resolved fluorescence lifetime spectrometer (Edinburg Instrument, Ltd.). The ultraviolet blocking performance of skin creams was evaluated using a UV transmittance analyzer (UV-2000s, Labsphere Co., Ltd.).

3. Results and Discussion

3.1. Structure and morphology characterization of the C-CDs

Representative TEM image of the C-CDs-120-30 is provided in Fig. 1(a), where spherical particles of high dispersity are apparently seen. The size distribution of the CDs is in the range of 2.4–5.6 nm, with an average size of 3.87 nm (inset). High-resolution TEM image clearly shows the existence of lattice stripes within particles (Fig. 1(b)). The lattice spacing is estimated to be 0.21 nm by measuring the distance between crystal planes, corresponding to the (1 0 0) facet of graphite [17]. This indicates the C-CDs possess sp^2 graphite-like structure. Raman spectrum of the carbon dots shows two prominent peaks at 1374 cm^{-1} and 1525 cm^{-1}, which are indexed to the well-known D band and G band of carbon

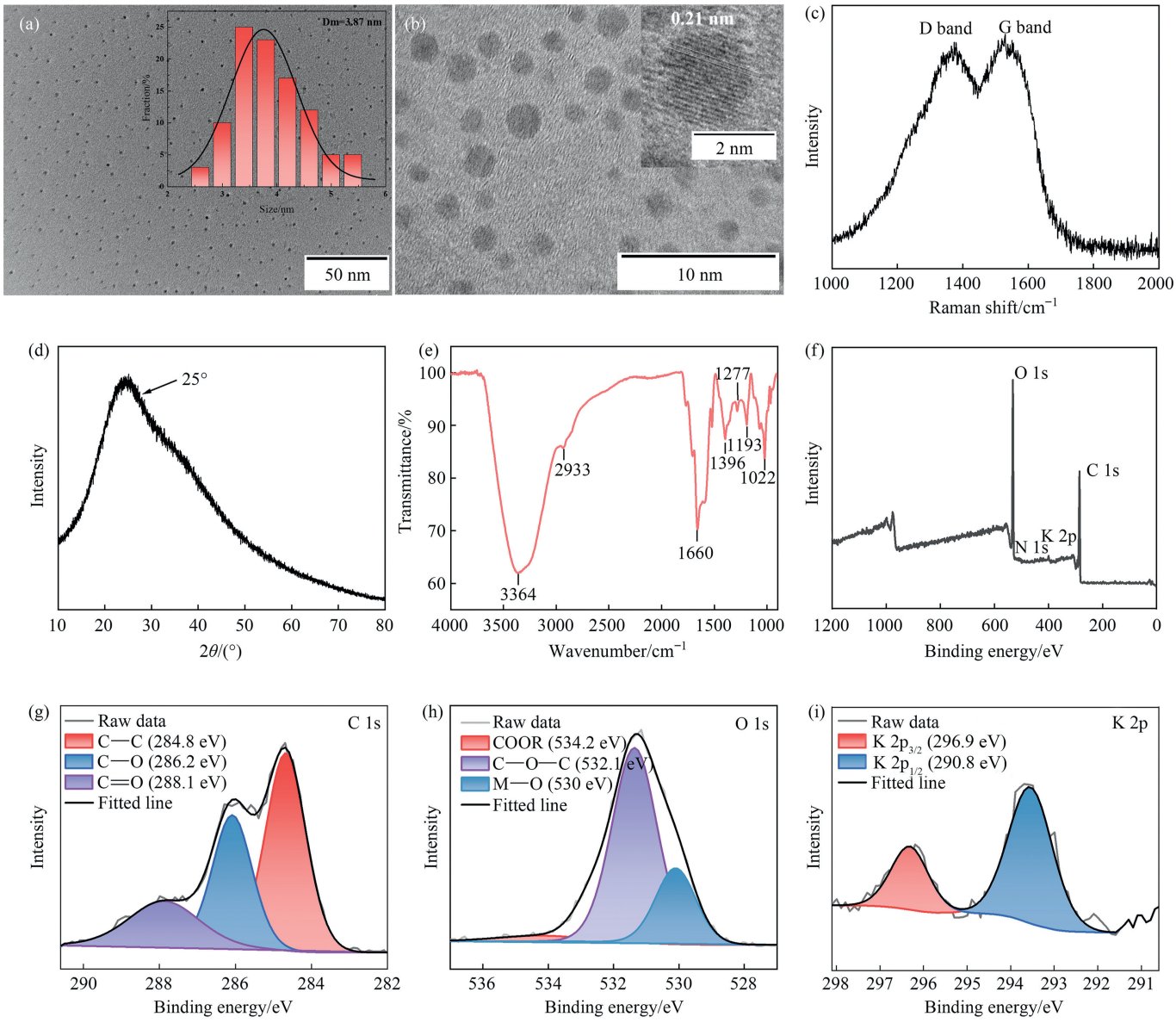

Fig. 1. (a) Representative TEM image of the C-CDs-120-30 (inset shows particle size distribution); (b) HRTEM image; (c) Raman spectrum; (d) XRD pattern; (e) FT-IR spectrum; (f) Full XPS spectrum; (g)–(i) High resolution XPS spectra of (g) C 1s; (h) O 1s; and (i) K 2p.

materials (Fig. 1(c)). The former one is associated with local defects or disorders in carbon, while the latter one is related to the graphitization characteristics of sp^2 carbon networks [18]. Fig. 1(d) shows the XRD pattern of C-CDs, in which a broad peak is observed at 2θ of 25°, without sharp diffraction peaks. The result reveals the derived C-CDs have low crystallinity [19].

The functional groups of the C-CDs-120-30 were firstly studied by FT-IR analysis (Fig. 1(e)). An intense broad absorption band appears at 3364 cm^{-1}, and is attributed to the O—H stretching vibration of the hydroxyl groups [20]. The band at 2933 cm^{-1} corresponds to the C—H stretching vibration in saturated hydrocarbons. The absorption bands at 1750 cm^{-1} and 1660 cm^{-1} are indexed to the C=O and C=C groups, respectively [21]. Besides, the bands at 1396 cm^{-1} and 1277 cm^{-1}/1022 cm^{-1} are related to C—OH and C—O—C groups [22]. The above spectral features indicate the microflow-prepared C-CDs have rich hydrophilic functional groups, which endow them with good dispersion and solubility in water. XPS characterization has been further applied to examine the chemical composition and bonding configuration of the C-CDs-120-30. The overall spectrum indicates the existence of C, O, K, and N elements, as reflected by the characteristic bands relating to C 1s (285 eV), O 1s (531 eV), K 2p (292 eV), and N1s (401 eV) (Fig. 1(f)) [23]. As we know, carrot juice has many nutrients, including fiber, potassium, nitrates, vitamins, *etc*. Thus, it is not surprising with the detection of the above elements. Chemical composition ratios for C, O, K, and N were measured to be 62.33%, 32.21%, 4.70% and 0.76%, respectively. Deconvolution of the C1s band suggests the presence of C—C/C=C (284.8 eV), C-O (286.2 eV), and C=O (288.1 eV) (Fig. 1(g)). As to the O1s spectrum (Fig. 1(h)), it can be deconvoluted into three subpeaks, which are assigned to the COOR (534.2 eV), C—O—C (532.1 eV), and M – O groups (530 eV). Spectral decomposition of the K2p peak derives two peaks at 290.8 eV (K $2p_{1/2}$) and 296.6 eV (K $2p_{3/2}$), revealing the co-existence of different spin states of electrons in the K 2p orbitals and the presence of K—O compounds. The above XPS results indicate the surface of the C-CDs has abundant functional groups.

3.2. Optical properties of C-CDs

CDs are well known to possess the ability to absorb light in the UV region while emitting light in the visible region. Fig. 2(a) shows the UV absorption and transmission spectra of the C-CDs solution with 0.4 mg·ml^{-1} of concentration in the range of 280–800 nm. In the absorption spectrum (black), two prominent absorption bands appear at 297 nm and 383 nm, corresponding to the π-π* transition of the carbon core and the *n*-π* transition of carbonyl groups, respectively [24]. This suggests the C-CDs contain aromatic structures and carbonyl functional groups. As to the transmission spectrum (red), near 0% UV transmittance is realized in the range of 280~400 nm, revealing the C-CDs have excellent UV absorption performance. However, for the carrot juice, no absorption bands are absorbed in the 280–400 nm of the UV absorption spectrum, confirming the successful generation of CDs from carrot juice (Fig. S2). The use of C-CDs provides several benefits, including easy availability, environmental friendliness, sustainability, and affordability. Furthermore, the color of the C-CDs solution changes from yellow to blue upon 365 nm UV irradiation, indicating their favorable optical properties (inset).

Fig. 2(b) provides the excitation spectrum as well as the emission spectra of the C-CDs under the excitation wavelength of 375–495 nm. The emission peak is gradually red shifted with the increase of the excitation wavelength. Such excitation-dependent photoluminescence behavior is a unique feature of CDs, and is ascribed to the multiple defect sites of CDs [25]. Specifically, the electron energy levels and transitions in CDs confer them photoluminescent properties, where different functional groups induce various electronic states. With varying excitation wavelengths, the energy gaps of certain functional groups will be initiated, and the corresponding surface defects become dominant. As a result, excitation-dependent emission behavior is presented. Fig. 2(c) shows the fluorescence lifetime decay curve of the C-CDs, which could be fitted with a multi-exponential equation as below:

$$I(t) = B_1 e^{(-\tau/\tau_1)} + B_2 e^{(-\tau/\tau_2)} + B_3 e^{(-\tau/\tau_3)} + B_4 e^{(-\tau/\tau_4)} \quad (1)$$

$$R_i = \frac{B_i}{\sum_{i=1}^{4} B_i} \quad (2)$$

$$\tau_{avg} = \sum_{i=1}^{4} R_i \tau_i \quad (3)$$

where $I(t)$ corresponds to the sum of the individual exponential decay intensities, B_i and τ_i are the amplitude and lifetime of each component, R_i is the fractional contribution of the decay lifetime of τ_i, τ_{avg} is the average fluorescence lifetime [26]. Fitting parameters were shown in Table S2. Resulting from the measurement, the average fluorescence lifetime was calculated to be 2.96 ns. Besides, the multi-exponential equation of the fluorescence lifetime decay curve indicates the luminescence of C-CDs is primarily related to the surface functional groups [26].

3.3. UV absorption of C-CDs

The influence of process parameters on the UV absorption property of the C-CDs was studied by regulating the reaction temperature and residence time. Once the reaction temperature increased from 110 °C to 120 °C, the intensity of the absorption bands at 297 nm and 383 nm concurrently enhanced, which should be due to the increased density of the C-CDs (Fig. 3(a)). However, when the reaction temperature exceeds 130 °C, the UV absorption intensity apparently decreased. Meanwhile, the color of the C-CDs solution became darker. This phenomenon can be explained by the enhanced carbonization degree of the C-CDs [27,28]. As reported, the carbonization of carbon dots often leads to the notorious aggregation-caused quenching effect as well as reduced UV absorption performance [29]. Same phenomenon was also observed for the C-CDs prepared at different residence times. Specifically, the absorption intensity of the C-CDs initially increased when the residence time was within 30 min, while gradually decreased at prolonged residence time (Fig. 3(b)). Once the reaction temperature or the residence time exceed certain values, the capillary can be easily blocked by the carbon dots. Therefore, C-CDs-120-30 were chosen for the subsequent experiments.

By recording the UV absorption spectra of the C-CDs-120-30 at different pH levels (2–12), the stability of the UV absorbance was evaluated. In acidic conditions, the absorption band at 383 nm is more pronounced than the band at 297 nm, indicating the C-CDs have better capability to block the UVA radiation (Fig. 3(c)). By contrast, in alkaline conditions, the absorption band at 297 nm became more prominent compared to the band at 383 nm (Fig. 3(d)). A reasonable explanation is that the UV absorption property of the C-CDs is closely related to their surface functional groups and chemical states. In acidic conditions, the carboxylic groups on the surface of C-CDs exist in a protonate form, where the C=O bonds containing a higher quantity of n electrons exhibiting increased polarity [30]. These electrons can be excited to the π* antibonding orbitals, leading to enhanced intensity of *n*-π* transitions at 383 nm. While in alkaline

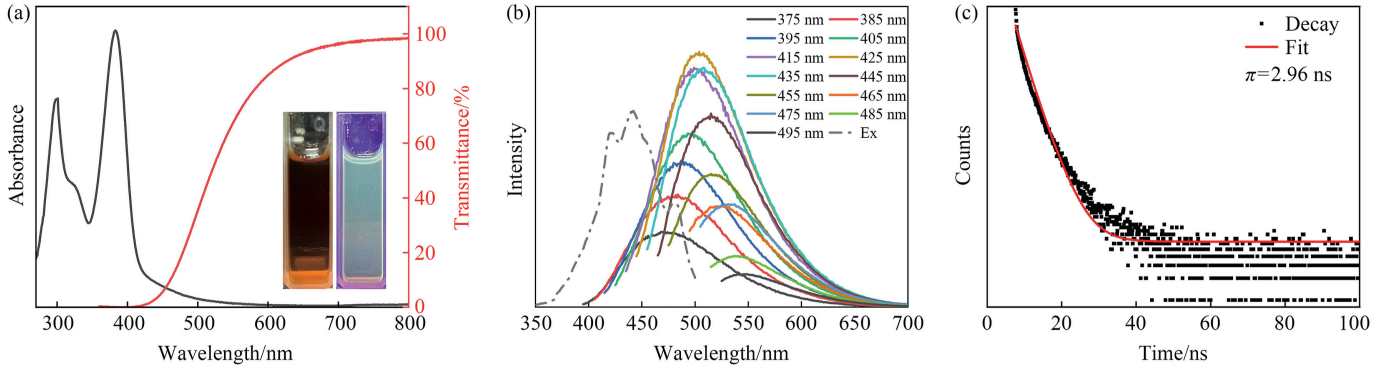

Fig. 2. (a) UV absorption and transmission spectra of the C-CDs-120-30, inset is a photograph of the CDs under natural light and 365 nm UV light; (b) excitation spectrum as well as emission spectra of the C-CDs-120-30 at different excitation wavelength; (c) fluorescence lifetime decay curve of the C-CDs-120-30.

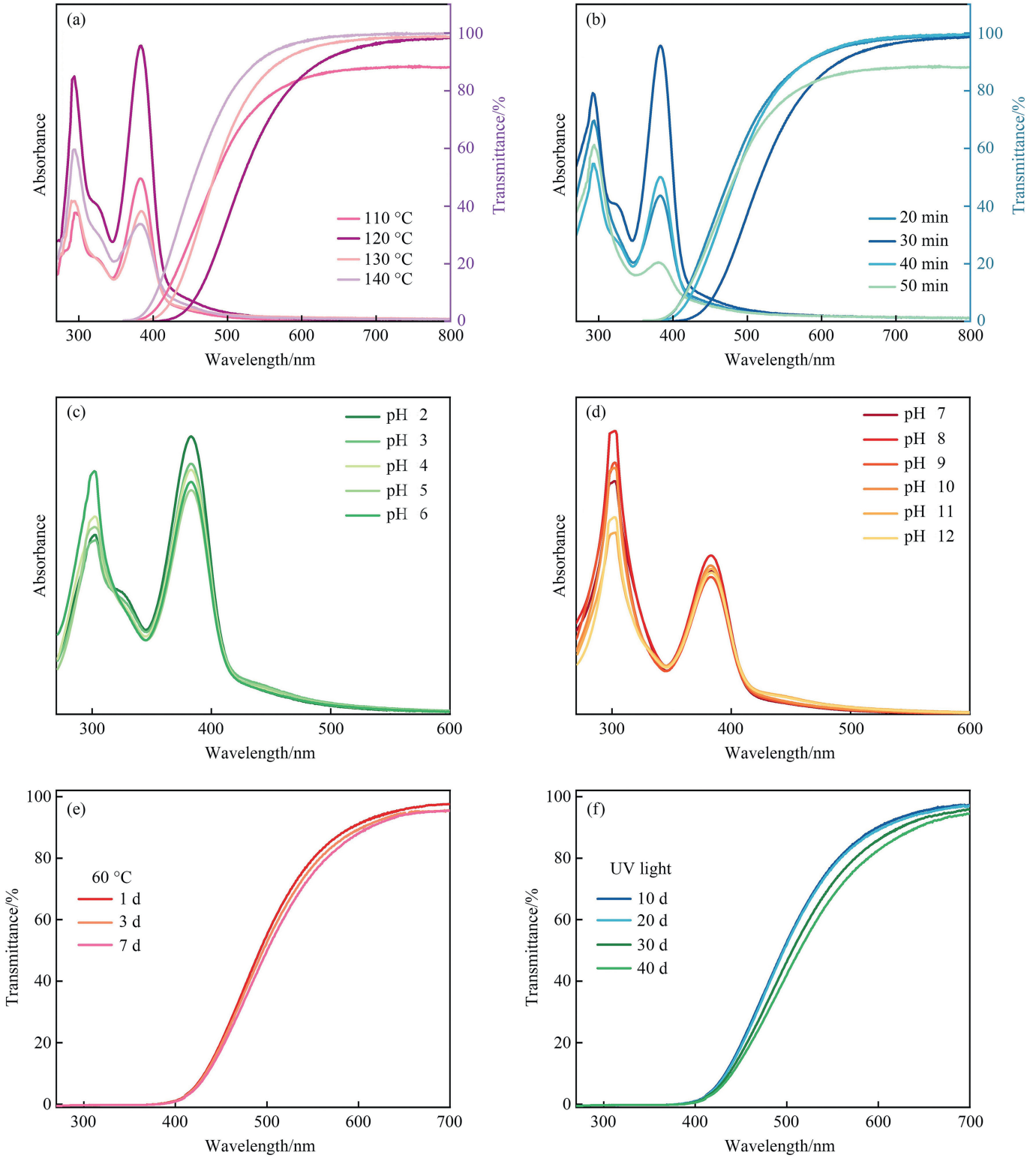

Fig. 3. UV-Vis absorption and transmission spectra of the C-CDs-120-30 obtained at: (a) different reaction temperatures; (b) different residence times; (c) acidic conditions (pH of 2–6); (d) Alkaline conditions (pH of 7–12); (e) transmission spectra of the C-CDs-120-30 preserved at 60 °C for 7 days; (f) Transmission spectra of the C-CDs-120-30 upon 365 nm UV irradiation for 40 days.

conditions, the carboxylic groups are predominantly in a deprotonate form, dispersing the n electrons with a negative charge, which decreases the probability of excitation to the π* antibonding orbitals and thus lowers the absorption intensity at 383 nm. Besides, it is also seen the UV absorbance intensity is rather stable in a wide range of pH, without shift in the peak position, suggesting the C-CDs can offer consistent UV protection over a broad pH range.

In addition to pH, the stability of UV absorbance of the C-CDs-120-30 was assessed at 60 °C for different times. The UV-Vis transmittance spectra remain virtually unchanged, even after 7 days, suggesting the C-CDs possess high temperature stability for UV absorbance (Fig. 3(e)). Furthermore, when exposed to 365 nm UV irradiation for 40 consecutive days, the C-CDs present slightly decrease in the transmittance in the range of 400–700 nm, while remained almost the same (close to 0%) within the 280–400 nm range (Fig. 3(f)). The results reveal the C-CDs have strong UV absorption ability and long-term stability. Therefore, the demonstrated excellent UV absorption performance of the C-CDs together with their good stability, biocompatibility and water solubility makes them an ideal candidate for sunscreen agent.

3.4. Application of C-CDs@PVA membrane

PVA is a non-toxic, biodegradable, and biocompatible polymer that has been widely used as packaging materials. However, it has been faced with a degradation challenge after long-term ultraviolet radiation, and therefore reducing its durability while in use [31]. The addition of UV absorbers into PVA is an effective manner to extend its useful life [32]. In this work, C-CDs of different concentrations were incorporated into PVA to prepare C-CDs@PVA films, which had similar thickness (Table S3), aiming to verify the strong UV absorption capability of the C-CDs. As depicted in Fig. 4(a), the PVA film without C-CDs has a UVA light transmission of 92.2% and UVB light transmission of 80.7%, suggesting it has poor ultraviolet resistance. By contrast, with the addition of C-CDs into the PVA film, the ultraviolet resistance greatly improves. Once the C-CDs concentration increases to 0.5 mg ml^{-1}, merely 7.8% UVA and 0.1% UVB can pass through the PVA film. As the C-CDs concentration further rises, the C-CDs@PVA film has enhanced UV-Vis absorption performance. Nearly 100% ultraviolet light can be blocked by the PVA films when the C-CDs concentration exceeds 1.0 mg ml^{-1}, and is accompanied by a significant reduction of visible light transmission (Fig. 4(b)). Meanwhile, the color of the C-CDs@PVA film changes from transparent to light yellow, and finally becomes brown with the elevated C-CDs concentration (Fig. S3). This is due to the fact that high concentration of C-CDs helps to enhance light scattering and absorption.

The UV blocking efficiency of the C-CDs@PVA films was also evaluated by a UV radiometer. Briefly, PVA and C-CDs@PVA1-5 films were placed on the substrate under natural light, with an initial UV light intensity of 1825 μW·cm^{-2}. The residual UV radiation intensity was then measured. As the C-CDs concentration raised from 0 to 0.5 mg·ml^{-1}, the UV blocking rate of the film increases from 4.8% to 97.3%, which can effectively prevent the UV damage to the films and extend their lifespan (Fig. 4(c)). The UV blocking efficiency of the films is measured again after sunlight exposure for 7 days. It is shown the PVA film without C-CDs only blocked 2.9% of UV radiation, in contrast to the excellent UV blocking performance of the C-CDs@PVA films. Moreover, the UV-

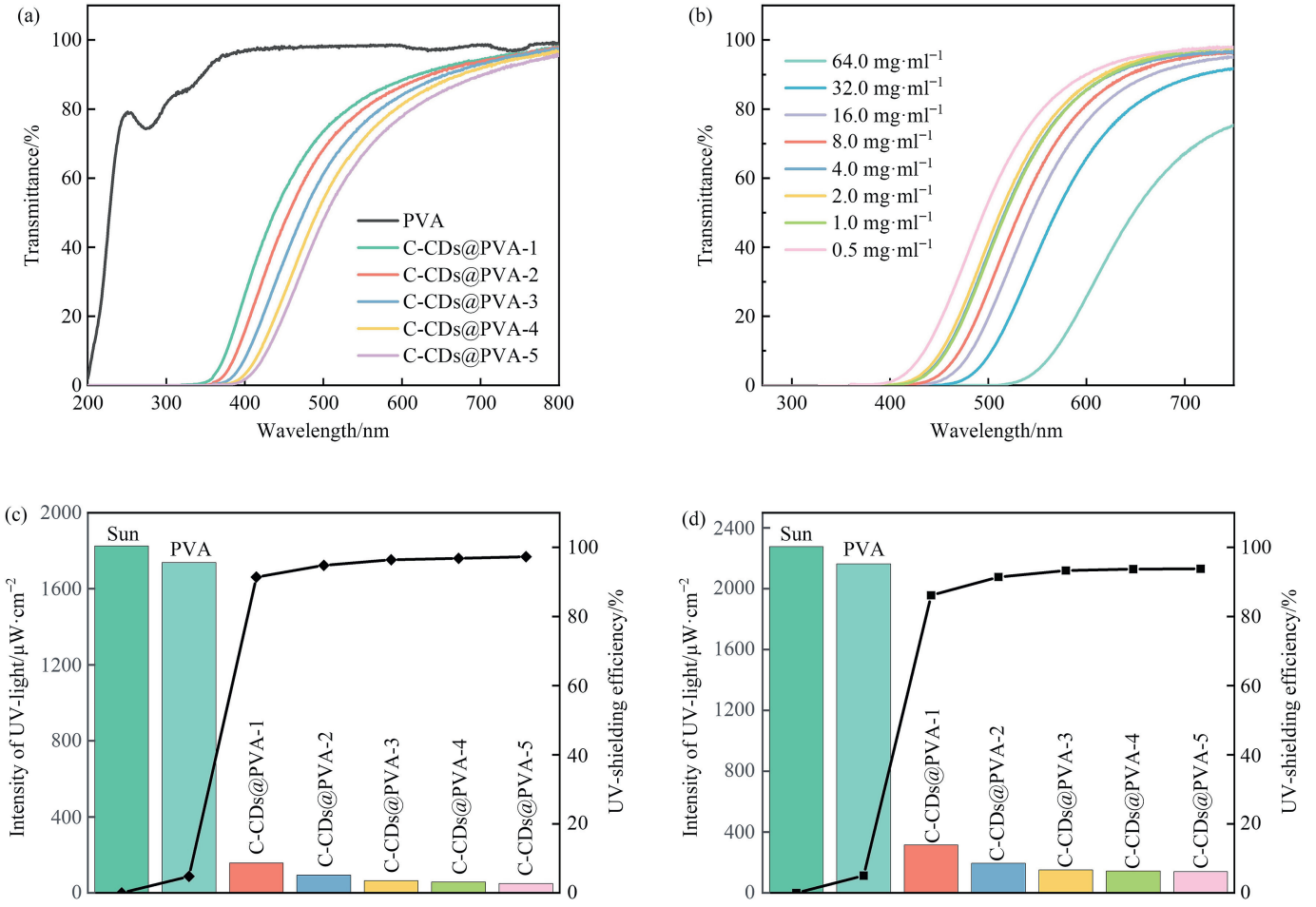

Fig. 4. UV transmission curves of the pure PVA film and C-CDs@PVA films: (a) C-CDs concentration: 0.1–0.5 mg·ml^{-1}; (b) C-CDs concentration: 0.5–64 mg·ml^{-1}; UV shielding efficiency of (c) the as-prepared C-CDs@PVA and (d) C-CDs@PVA films after sunlight exposure for 7 days.

shielding efficiency of the C-CDs@PVA1-5 films is measured to be 86.1%, 91.4%, 93.3%, 93.7%, and 93.8%, respectively, suggesting their stability in blocking UV radiation (Fig. 4(d)). The above results reveal the C-CDs@PVA films possess excellent UV-shielding performance and anti-photoaging properties, making them appealing for UV radiation protection purpose.

In addition, this work also prepared PVA film as well as C-CDs@PVA films of different film thickness (30–150 μm), and studied the influence of film thickness on its sun protection performance. Fig. S4 shows UV transmittance spectra of PVA films and C-CDs@PVA films of different thickness. For both films, UV transmittance decreases with the increase of film thickness. Compared to PVA films, C-CDs@PVA films have better UV absorption performance, where the transmittance of UV at 320 nm decreases from 43.3% to 2.1% when the film thickness increases from 30 μm to 150 μm. Therefore, the film thickness can affect the sun protection performance of PVA films and C-CDs@PVA films. The UV light protection mechanism of C-CDs@PVA membrane can be attributed to two aspects: C-CDs and PVA film. As we known, the surface of C-CDs contains functional groups like aromatic and carbonyl groups. They can absorb ultraviolet light and cause π-π* and *n*-π* transitions. Besides, the PVA films also exhibit UV-shielding performance. Both factors contribute to UV light protection.

To better demonstrate the UV-blocking property of the C-CDs@PVA films, the C-CDs solution was exposed to a UV lamp (365 nm) for irradiation, in which a PVA-based film was placed

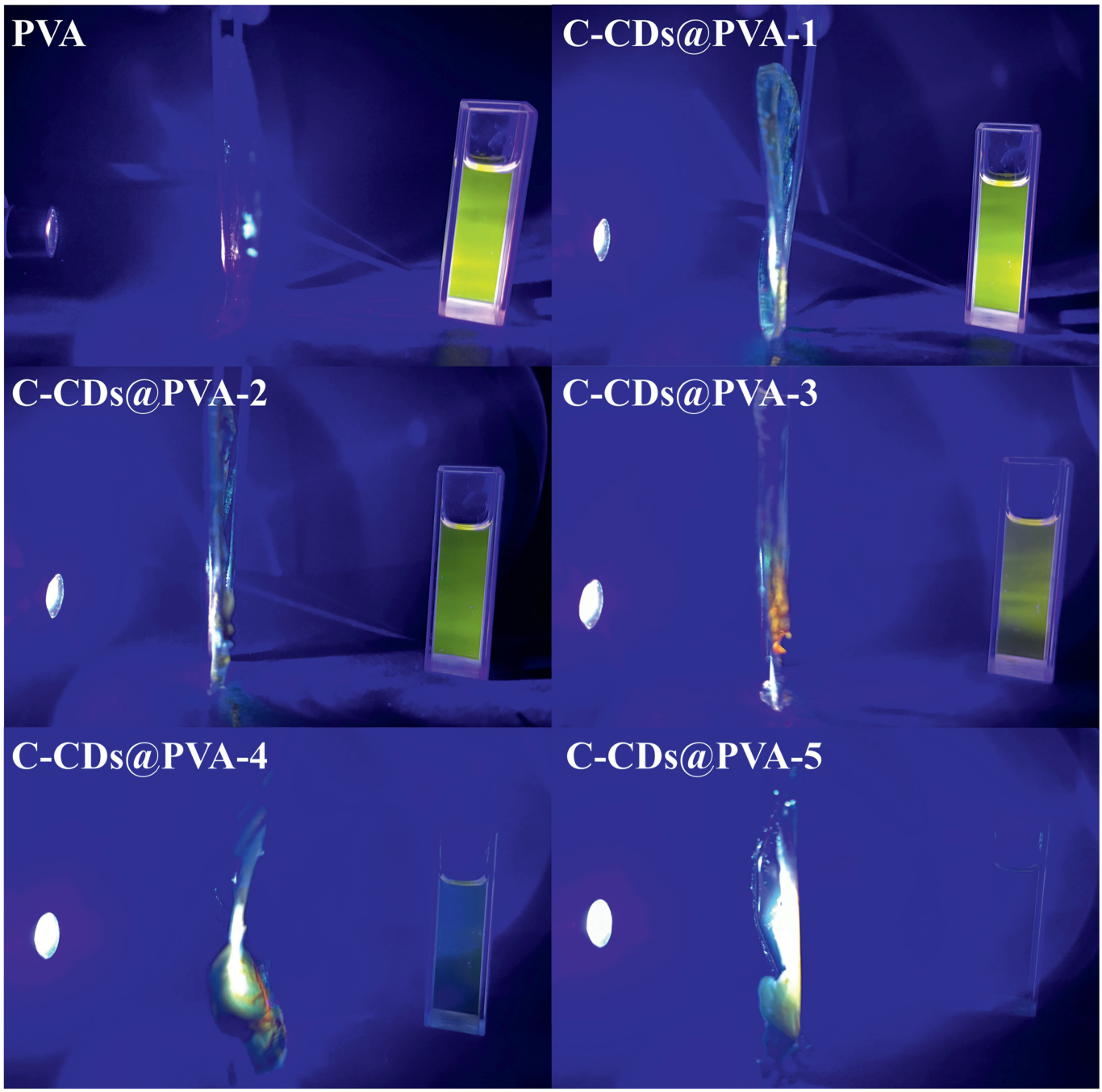

Fig. 5. Photographs of C-CDs solutions upon 365 nm UV irradiation, between which C-CDs@PVA films are placed.

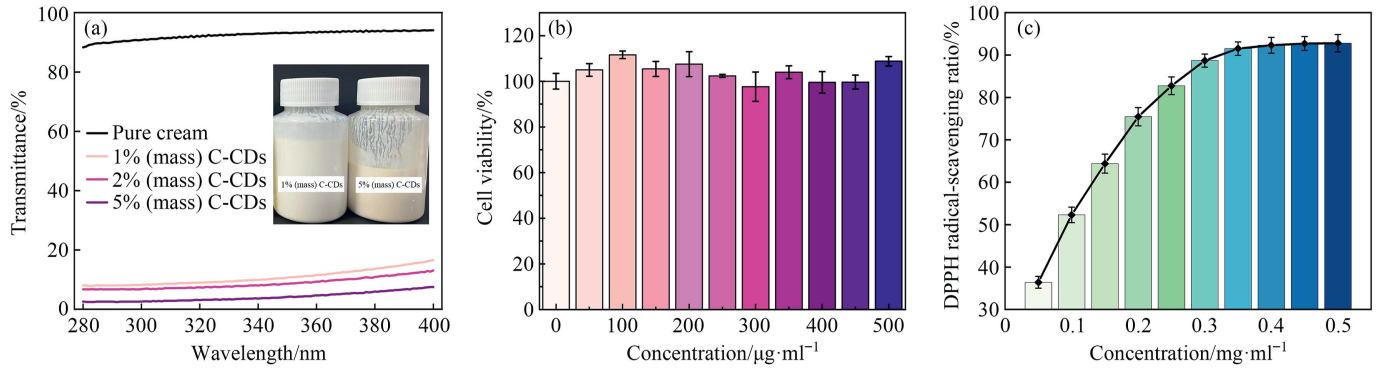

Fig. 6. (a) UV transmittance spectra of skin cream with different concentrations of the C-CDs; (b) In vitro cytotoxic effects of the C-CDs on HFF cells at different concentrations; (c) Scavenging activity of the C-CDs against DPPH free radicals at varying concentrations.

between them to absorb UV light. One can see the C-CDs solution emits bright yellow fluorescence with the pure PVA film. However, as the C-CDs concentration in the film increases, the fluorescence from the C-CDs solution gradually weakens. For the C-CDs solutions filtered by the C-CDs@PVA-4 and C-CDs@PVA-4, yellow fluorescence is hardly seen (Fig. 5). This in turn, suggests the addition of the C-CDs in the PVA film will endow it with UV-shielding property.

3.5. Practical application of the C-CDs in sunscreen

To assess the practical application of the C-CDs in sunscreen creams, they were added as an ingredient in a representative skin cream formulation. The skin cream without C-CDs has only slight UV-shielding effect, as reflected by the high transmittance of ultraviolet rays (~90%) in the range of 280–400 nm (Fig. 6(a)). By contrast, the addition of the C-CDs in the skin cream leads to drastically reduced UV transmittance. Specifically, for the skin cream with 1% (mass) C-CDs, the average transmittance in the UVB and UVA range is 8.3% and 12%, respectively, which is much lower compared to the pure cream. As to the skin cream with 5% (mass) C-CDs, the average transmittance is measured to be 2.7% and 4.9% in the UVB and UVA regions, and can effectively protect people from UV irradiation. In addition, UV spectra of skin creams containing 1% (mass) of commercial sunscreen agents (EMHC and DHHB) were also recorded (Fig. S5). For the skin cream with 1% (mass) of EMHC, the average transmittance in the UVB and UVA range is 30% and 87%. As to the skin cream containing 1% (mass) of DHHB, the average transmittance was measured to be 48% and 24%. The above results indicate the C-CDs have better UV absorption performance than commercial sunscreen agents, and can significantly reduce UV transmittance in UVA and UVB regions. Cytotoxicity of C-CDs is an important safety assessment parameter, and is also evaluated against HFF cells using the MTT assay in our work. As shown in Fig. 6(b), the viability of HFF cells remained above 97% after a 48-h incubation with the C-CDs, revealing their excellent biocompatibility.

In addition to the UV-shielding effect, the phenolic hydroxyl groups of C-CDs also endow them with the ability to scavenge free radicals [33]. In this work, the 2,2-diphenylpicrylhydrazyl (DPPH) assay has been used to evaluate the properties of the C-CDs for scavenging free radicals. As shown in Fig. 6(c), with the increase of the C-CDs concentration, the scavenging activity of the C-CDs on DPPH free radicals continues to rise, which exceeds 90% when the concentration of the C-CDs reaches 0.5 mg ml^{-1}. The results reveal the C-CDs serve as potential antioxidants for the scavenging of free radicals.

4. Conclusions

In conclusion, this work demonstrates a green continuous microflow approach for the synthesis of carbon dots from carrot juice. The composition, morphology, structure, size, and optical properties of the C-CDs have been examined by complementary characterization, with the process parameters explored and optimized. Small sized carbon dots (averaged size: 3.87 nm) of narrow size distribution and good water solubility prove to be synthesized, and their surfaces have abundant functional groups. The optical properties of the C-CDs were studied, suggesting they have excellent ultraviolet absorption performance in both UVA and UVB regions. Besides, the UV absorption property of the C-CDs is rather stable in a wide range of pH, even after 7 days or in a relative high temperature of 60 °C. This indicates the C-CDs can offer consistent UV protection in harsh conditions. By incorporating the C-CDs in PVA films to form C-CDs@PVA composites, they can endow the PVA films with UV absorption property. Nearly 100% ultraviolet light can be blocked by the PVA films once the concentration of the C-CDs exceeds 1.0 mg ml^{-1}.

The practical application of the C-CDs has been further evaluated by adding them in skin cream as sunscreen agents. With the increased concentration of the C-CDs, the cream has significantly enhanced UV absorption properties. Merely 4.9% and 2.7% ultraviolet light is transmitted in UVA and UVB regions when the concentration of the C-CDs reaches 5% (mass). Compared to commercial sunscreen agents like EMHC and DHHB, the C-CDs exhibit better UV absorption performance. Besides, the C-CDs also demonstrate good biocompatibility against HFF cells as well as high DPPH radical scavenging activity. These properties make them appealing as effective and green sunscreen absorbers. The green continuous microflow approach for the synthesis of C-CDs, together with their excellent UV absorption properties and good biocompatibility, is expected to promote the development of natural sunscreen agents.

CRediT Authorship Contribution Statement

Ziyang Li: Writing – original draft, Investigation, Formal analysis. Zhikun Miao: Validation, Methodology, Investigation, Formal analysis. Jie Shen: Validation, Software, Formal analysis. Jing Wang: Writing – review & editing, Writing – original draft, Resources, Investigation. Liangliang Lin: Writing – review & editing, Writing – original draft, Supervision, Project administration, Funding acquisition, Conceptualization.

Data Availability

Data will be made available on request.

Declaration of Competing Interest

The authors declare that they have no known competing financial interests or personal relationships that could have appeared to influence the work reported in this paper.

Acknowledgements

We would like to acknowledge the financial support from National Natural Science Foundation of China (22078125), Postdoctoral Science Foundation of China (2023M741472), and Fundamental Research Funds for the Central Universities (JUSRP622038).

Supplementary Material

Supplementary data to this article can be found online at https://doi.org/10.1016/j.cjche.2024.10.008.

References

[1] R. Farouk, E.A. El-Kharadly, A.H.M. Elwahy, H.I. Ibrahim, A.A. Mousa, Synthesis of new reactive dyes containing commercial UV-absorbers with enhanced simultaneous dyeing and anti-UV properties for cotton fabric, *J. Indian Chem. Soc.* 98 (2) (2021) 100022.
[2] N. Serpone, D. Dondi, A. Albini, Inorganic and organic UV filters: their role and efficacy in sunscreens and suncare products, *Inorg. Chim. Acta.* 360 (3) (2007) 794–802.
[3] E. Gilbert, F. Pirot, V. Bertholle, L. Roussel, F. Falson, K. Padois, Commonly used UV filter toxicity on biological functions: review of last decade studies, *Int. J. Cosmet. Sci.* 35 (3) (2013) 208–219.
[4] T.H. Kim, S.H. Park, S. Lee, A.V.S.L.S. Bharadwaj, Y.S. Lee, C.G. Yoo, T.H. Kim, A review of biomass-derived UV-shielding materials for bio-composites, *Energies* 16 (5) (2023) 2231.
[5] M.A. Darmawan, N.H. Ramadhani, N.A. Hubeis, M.Y.A. Ramadhan, M. Sahlan, S. Abd-Aziz, M. Gozan, Natural sunscreen formulation with a high Sun protection factor (SPF) from tengkawang butter and lignin, *Ind. Crops Prod.* 177 (2022) 114466.
[6] S.S.K. Wijeratne, M.M. Abou-Zaid, F. Shahidi, Antioxidant polyphenols in almond and its coproducts, *J. Agric. Food Chem.* 54 (2) (2006) 312–318.
[7] H. Zhang, X.X. Liu, S.Y. Fu, Y.C. Chen, High-value utilization of kraft lignin: color reduction and evaluation as sunscreen ingredient, *Int. J. Biol. Macromol.* 133 (2019) 86–92.
[8] R. Mansuri, A. Diwan, H. Kumar, K. Dangwal, D. Yadav, Potential of natural compounds as sunscreen agents, *Pharm. Rev.* 15 (29) (2021) 47–56.
[9] L.S. Zhang, Y.D. Ji, W.D. Li, B. Zhang, Q. Ma, B.W. Qin, Y.L. Zhang, D. Yue, Z.L. Wang, Enhancing luminescence of AF_2: Ln^{3+} (A=Ca, Sr; Ln = Eu, Tb) by the use of carbon dots, *Ceram. Int.* 50 (16) (2024) 28967–28977.
[10] J. Shen, X.J. Zheng, L.L. Lin, H.J. Xu, G.H. Xu, Reaction time-controlled synthesis of multicolor carbon dots for white light-emitting diodes, *ACS Appl. Nano Mater.* 6 (4) (2023) 2478–2490.
[11] L.L. Lin, Y. Xia, H.Y. Wen, W.T. Lu, Z.Y. Li, H.J. Xu, J. Zhou, Green and continuous microflow synthesis of fluorescent carbon quantum dots for bio-imaging application, *AIChE J.* 69 (1) (2023) e17901.
[12] A.S. Patil, R.D. Waghmare, S.P. Pawar, S.T. Salunkhe, G.B. Kolekar, D. Sohn, A.H. Gore, Photophysical insights of highly transparent, flexible and re-emissive PVA@WTR-CDs composite thin films: a next generation food packaging material for UV blocking applications, *J. Photochem. Photobiol. Chem.* 400 (2020) 112647.
[13] Y.L. Xu, Z.Q. Xu, C.C. Chen, W.H. Ye, B.Y. Guo, J.M. Qiu, J.L. Zhuang, C.F. Hu, B.F. Lei, G.Q. Hu, Y.L. Liu, Synthesis of nitrogen-doped carbon dots with 3-aminoquinoline and citric acid as an absorbent in full ultraviolet bands and application of transparent sunscreen umbrella, *Dyes Pigments* 214 (2023) 111204.
[14] X.M. Zhu, W.T. Qi, M. Wang, S.X. Zhan, X.Z. Liu, Y.T. Zhao, V. Hessel, Z.H. Chen, L.L. Lin, Microfluidic steam-based synthesis of luminescent carbon quantum dots as sensing probes for nitrite detection, *Green Process. Synth.* 12 (1) (2023) 20228144.
[15] Z.Y. Li, L.L. Lin, J. Shen, C.D. Li, K.K. Ostrikov, Microflow synthesis of fluorescent carbon dots for selective Co^{2+} detection, *Ind. Eng. Chem. Res.* 63 (10) (2024) 4420–4429.
[16] R. Sahana, S.C.G. Kiruba Daniel, S.G. Sankar, G. Archunan, S.J. Vennison, M. Sivakumar, Formulation of bactericidal cold cream against clinical pathogens using *Cassia auriculata* flower extract-synthesized Ag nanoparticles, *Green Chem. Lett. Rev.* 7 (1) (2014) 64–72.
[17] Z. Tian, X.T. Zhang, D. Li, D. Zhou, P.T. Jing, D.Z. Shen, S.N. Qu, R. Zboril, A.L. Rogach, Full-color inorganic carbon dot phosphors for white-light-emitting diodes, *Adv. Opt. Mater.* 5 (19) (2017) 1700416.
[18] X.H. Li, W.D. Wang, W.F. Dong, X.X. Zhang, H.J. Xu, L.L. Lin, Plasma-liquid synthesized carbon-supported platinum nanoparticles as active electrocatalysts, *J. Taiwan Inst. Chem. Eng.* 133 (2022) 104234.
[19] W.I. Singh, S. Sinha, N.A. Devi, S. Nongthombam, S. Laha, B.P. Swain, Investigation of chemical bonding and electronic network of rGO/PANI/PVA electrospun nanofiber, *Polym. Bull.* 78 (11) (2021) 6613–6629.
[20] X.H. Li, C.X. Zhao, L.L. Lin, Plasma-based instant synthesis of functionalized gold nanoparticles for colorimetric detection of lead ions, *Chem. Eng. Sci.* 260 (2022) 117849.
[21] X.T. Ma, S.R. Li, V. Hessel, L.L. Lin, S. Meskers, F. Gallucci, Synthesis of luminescent carbon quantum dots by microplasma process, *Chem. Eng. Process. Process. Intensif.* 140 (2019) 29–35.
[22] Q.H. Pho, L.L. Lin, N.N. Tran, T.T. Tran, A.H. Nguyen, D. Losic, E.V. Rebrov, V. Hessel, Rational design for the microplasma synthesis from vitamin B9 to N-doped carbon quantum dots towards selected applications, *Carbon* 198 (2022) 22–33.
[23] X.Y. Wang, M.Y. Lu, J. Ma, P. Ning, L. Che, Synthesis of K-doped g-C_3N_4/carbon microsphere@graphene composite with high surface area for enhanced adsorption and visible photocatalytic degradation of tetracycline, *J. Taiwan Inst. Chem. Eng.* 91 (2018) 609–622.
[24] P. Singhal, B.G. Vats, V. Pulhani, Origin of solvent and excitation dependent emission in newly synthesized amphiphilic carbon dots, *J. Lumin.* 244 (2022) 118742.
[25] C. Wei, S. Hu, F.X. Liang, Z.N. Song, X. Liu, One-pot synthesis of concentration and excitation dual-dependency truly full-color photoluminescence carbon dots, *Chin. Chem. Lett.* 33 (8) (2022) 4116–4120.
[26] Y.J. Zhao, L.X. Yu, Y.K. Deng, K.L. Peng, Y. Yu, X.L. Zeng, A multi-color carbon quantum dots based on the coordinated effect of quantum size and surface defects with green synthesis, *Ceram. Int.* 49 (11) (2023) 16647–16651.
[27] Y. Zhang, Y.L. Wang, X.T. Feng, F. Zhang, Y.Z. Yang, X.G. Liu, Effect of reaction temperature on structure and fluorescence properties of nitrogen-doped carbon dots, *Appl. Surf. Sci.* 387 (2016) 1236–1246.
[28] S.S. Xue, P.F. Li, L. Sun, L. An, D. Qu, X.Y. Wang, Z.C. Sun, The formation process and mechanism of carbon dots prepared from aromatic compounds as precursors: a review, *Small* 19 (31) (2023) e2206180.
[29] Y.Q. Zhang, P. Zhuo, H. Yin, Y. Fan, J.H. Zhang, X.Y. Liu, Z.Q. Chen, Solid-state fluorescent carbon dots with aggregation-induced yellow emission for white light-emitting diodes with high luminous efficiencies, *ACS Appl. Mater. Interfaces* 11 (27) (2019) 24395–24403.
[30] H. Ehtesabi, Z. Hallaji, S. Najafi Nobar, Z. Bagheri, Carbon dots with pH-responsive fluorescence: a review on synthesis and cell biological applications, *Microchim. Acta* 187 (2) (2020) 150.
[31] D.N. Wang, Y.J. Gu, S. Feng, W.S. Yang, H.Q. Dai, H.N. Xiao, J.Q. Han, Lignin-containing biodegradable UV-blocking films: a review, *Green Chem.* 25 (22) (2023) 9020–9044.
[32] A.A. Abdel-Fattah, Y.S. Soliman, Performance improvement of pentacosadiynoic acid label dosimeter for radiation processing technology, *Radiat. Phys. Chem.* 141 (2017) 66–72.
[33] D. Villaño, M.S. Fernández-Pachón, M.L. Moyá, A.M. Troncoso, M.C. García-Parrilla, Radical scavenging ability of polyphenolic compounds towards DPPH free radical, *Talanta* 71 (1) (2007) 230–235.